34th Annual International Conference of the IEEE EMBS
San Diego, California USA, 28 August - 1 September, 2012

Volumetric Imaging Using Single Chip Integrated CMUT-on-CMOS IVUS Array

Coskun Tekes, Jaime Zahorian, Gokce Gurun, Sarp Satir, Toby Xu, Michael Hochman, F. Levent Degertekin

Abstract— **An intravascular ultrasound (IVUS) catheter that can provide forward viewing volumetric ultrasound images would be an invaluable clinical tool for guiding interventions. Single chip integration of front-end electronics with capacitive micromachined ultrasonic transducers (CMUTs) is highly desirable to reduce the interconnection complexity and enable miniaturization in IVUS catheters. For this purpose we use the monolithic CMUT-on-CMOS integration where CMUTs are fabricated directly on top of pre-processed CMOS wafers. This minimizes parasitic capacitances associated with connection lines. We have recently implemented a system design including all the required electronics using 0.35-µm CMOS process integrated with a 1.4-mm diameter CMUT array. In this study, we present the experimental volumetric imaging results from an ex-vivo chicken heart phantom. The imaging results demonstrate that the single-chip forward looking IVUS (FL-IVUS) system with monolithically integrated electronics has potential to visualize the front view of coronary arteries.**

I. Introduction

Intravascular ultrasound (IVUS) is a useful tool for diagnosing arterial diseases, guiding interventions such as stent deployment and monitoring ablation procedures [1]. Currently available IVUS systems are side looking (SL) catheter probes and provide 2-D cross-sectional images of the vessel. A significant shortcoming of these SL probes is the lack of forward looking (FL) capability to provide true volumetric images in front of the catheter. Therefore, an IVUS catheter that can provide FL volumetric ultrasound images would be an invaluable clinical tool for guiding interventions in coronary arteries especially for treatment of chronic total occlusions (CTOs) and for helping stent deployment.

Designing a FL-IVUS system is challenging since IVUS catheters need to be as small as 1 mm in diameter in order to move inside narrowest vessels and hence the transducer area is limited by the catheter's front tip. Moreover, a central opening is required to enable for a guide wire to pass through. On the other hand, in order to provide volumetric imaging, the transducer array needs to be a two dimensional array. Therefore, a ring-shaped transducer array is a suitable configuration for FL-IVUS [2, 3]. The small-sized catheter strictly limits the number of cables for communicating with the external processing unit. In addition, the front-end must be very simple to fit onto the probe. Due to these constraints, IVUS systems should involve synthetic phased array processing. In other words, the array channels must be multiplexed in multiple firing events to simplify the front end and cable count.

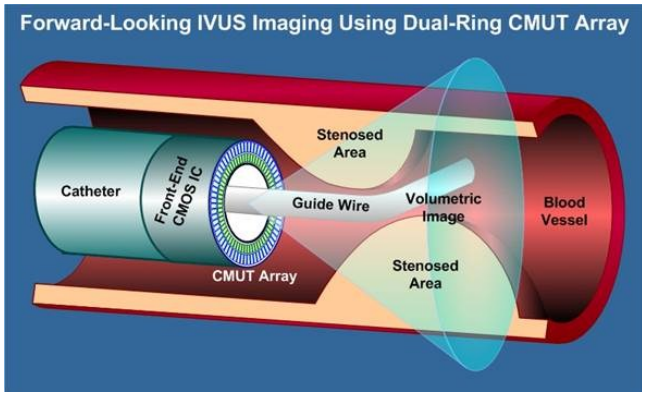

Figure 1. Conceptual drawing of a single-chip fully-integrated FL-IVUS imaging catheter based on a dual-ring CMUT array monolithically integrated with the complete front-end CMOS IC

Although piezoelectric transducers are commonly used in IVUS catheters, the small sizes result in extremely small transducer elements which can be very difficult to fabricate with current piezoelectric technology. Recent efforts show that capacitive micromachined ultrasonic transducer (CMUT) technology is promising for FL-IVUS imaging since it offers high bandwidth, good sensitivity and flexibility to fabricate arrays of different shapes and sizes [4, 5]. In addition, it enables monolithic or flip-chip-bonding integration of front-end electronics. By taking advantage of the flexibility offered by CMUT technology, it is possible to utilize the area around the guide wire efficiently by implementing very complex array structures for FL-IVUS imaging.

We have recently fabricated a single-chip FL-IVUS system design using the monolithic CMUT-on-CMOS integration where dual ring CMUT arrays are fabricated directly on top of pre-processed CMOS wafers (Fig. 1) [6-8]. In this study, we demonstrate the volumetric imaging capability of the FL-IVUS using an ex-vivo chicken heart phantom. In the following sections, we present the CMUT and integrated electronic design, characterization of CMUT array, data acquisition and image reconstruction, and experimental results.

* This work was supported by NIH grants R01 EB010070 and R01 HL082811.

The authors are with George W. Woodruff School of Mechanical Engineering, Georgia Institute of Technology, Atlanta, GA 30332-0405 USA (e-mail: coskun.tekes@me.gatech.edu).

II. METHODS

A. CMUT Array Design

The micrograph of the single chip system including the dual ring CMUT arrays monolithically fabricated on top of the CMOS IC is shown in Fig. 2-right. The arrays used for the imaging experiments have 56 transmit (outer ring) and 48 receive (inner ring) elements with 1.31 mm and 1.13 mm center diameters, respectively. The array elements contain 4 individual membranes and are approximately 70 µm × 70 µm in size. These devices were fabricated to operate at a center frequency of 20 MHz and have a collapse voltage of 240 V. Table I summarizes the fabricated CMUT array parameters.

TABLE I. CMUT ARRAY PARAMETERS

Number of elements	56 Tx – 48 Rx
Center Frequency	20 MHz
Element Pitch	70 x 70 µm
Outer diameter	1.4 mm
Isolation layer thickness	0.21 µm
Total membrane thickness	2.3 µm
Gap thickness	0.12 µm

B. Monolithically Integrated Electronics

Fig. 2-left shows a micrograph of the integrated circuit (IC). It is designed using 0.35-µm CMOS process and includes 56 pulsers capable of generating 25-V unipolar pulses and a low-noise receiver transimpedance amplifier (TIA) for each of the 48 CMUT array elements. The chip also includes multiplexers, buffers and a digital control circuitry that is designed to synchronize transmitting and receiving sequence during the data acquisition.

All of the active circuitry and the CMUT array fit into a size of 1.5-mm diameter silicon donut with a 430-µm gap left inside for a guide wire. The system requires a total of 13 external connections including IC feeding voltages, 4-channel output, digital control signals and CMUT bias voltages. The total power consumption of the chip is around 20 mW. The receive TIAs have 630-kΩ gain with 25-MHz bandwidth.

C. Experimental Setup

To demonstrate imaging performance of FL dual ring CMUT arrays, a custom data collection setup was constructed. Fabricated CMUT array is first wirebonded to a ceramic dual inline package (DIP) chip holder with 13 connections and a small petri dish which has a hole in the bottom is glued on the top of the chip holder. The dish is filled with vegetable oil so that custom phantoms can be immersed in the oil. The chip holder is placed in a custom PCB that all data acquisition and control signal connections are performed. The output receive channels are digitized

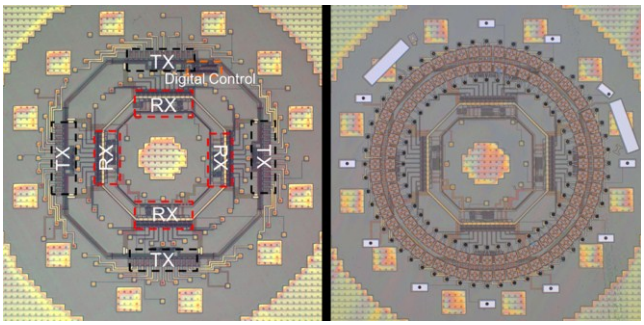

Figure 2. Micrograph of the IC with receive and transmit electronics and the digital control circuitry (left). Monolithically fabricated dual ring CMUT array with 56 Tx and 48 Rx elements (right).

using 2 digitizer cards (Spectrum UltraFast M3i.4142) which have 14-bit ADCs and 250 MS/s sampling rate. The clock signal for the digital control of the IC is generated by the external digital I/O of the digitizer card. During each clock signal a transmit (Tx) element is fired and 4 parallel receive (Rx) output channels are digitized simultaneously and saved for further data processing and image reconstruction.

III. RESULTS

A. Pulse-Echo Response

We performed pulse-echo experiments from an oil-air interface at nearly 10 mm above the CMUT to characterize the performance of the array elements. We collected RF A-scans from all Tx-Rx element combinations. Both Tx and Rx arrays were operated in conventional mode at 90% of collapse voltage (240V). We used 25-V unipolar and 30-ns width pulses as the excitation. We processed the raw RF A-scan data by a digital band-pass filter with a 10-30 MHz pass-band to eliminate out-of-band noise. Since the attenuation of ultrasound in oil dramatically increases with frequency, we applied 16 averaging to increase SNR.

Fig. 3 shows pulse-echo and frequency response of a single CMUT array element. The pulse-echo response from the oil-air interface has a main echo and following echos due to crosstalk between array elements. These following echos have signal level of more than 15 dB lower than the main echo. As expected the frequency response shows 20 MHz center frequency with a nearly 50% 6-dB fractional bandwidth. These values are maintained as the same throughout the array elements with a slight variation. The averaged computed pulse-echo SNR for all Tx-Rx element combinations is 24 dB.

B. Image Reconstruction

In image reconstruction, we first recorded all A-scans obtained from 56×48 Tx-Rx combinations to further perform offline processing and beamforming. Since the effective imaging depth is 10 mm, we collected 25-µs data for each A-scan with a sampling rate of 250 MS/s and pulse repetition of 40 kHz. Note that sufficient amount of time is reserved for the successive pulse-echo operations to ensure the travelling

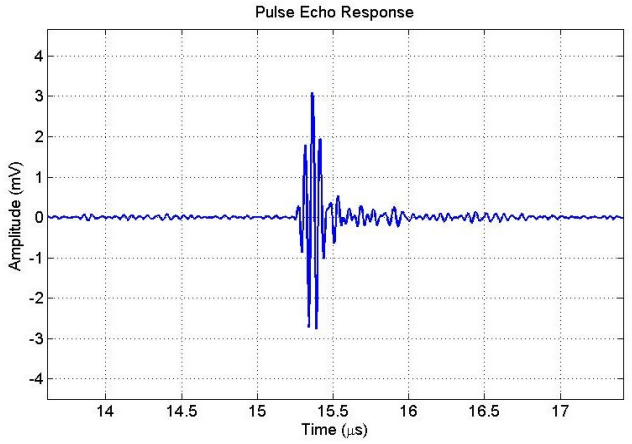

(a)

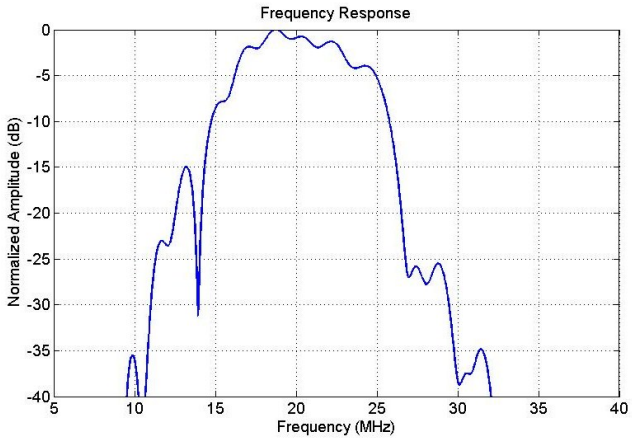

(b)

Figure 3. (a) Pulse-Echo and (b) Frequency response of a single CMUT array element.

waves inside the medium are totally attenuated. Thus, the latter pulse-echo events are not distorted by the formers.

A custom RF beamforming software was written to process A-scan data. We first filtered each data set using a digital band-pass filter described above. Then, we applied synthetic phased array beamforming using standard delay-and-sum method to calculate the image intensity in each image voxel by using dynamic transmit and receive focusing [3]:

$$I(u) = \sum_{i=1}^{N_t} \sum_{j=1}^{N_r} w_a(i,j) w_n(i,j) s_{ij}(m), \qquad (1)$$

where u is the 3-D cartesian coordinates of the image voxel as *(x,y,z)*; *s(.)* is the sampled RF A-scan; m is the sample index corresponding to the total flight time in terms of number of sample; w_a is the apodization coefficient; w_n is the Norton's weightings coefficient for ring array apertures; the first and second sums are over the N_t transmit and N_r receive elements, respectively; f_s is the sampling frequency; and c is the sound velocity in oil. The sample index m is calculated as:

$$m = round\left\{(|u - u_i| + |u - u_j|) \cdot \frac{f_s}{c}\right\}, \qquad (2)$$

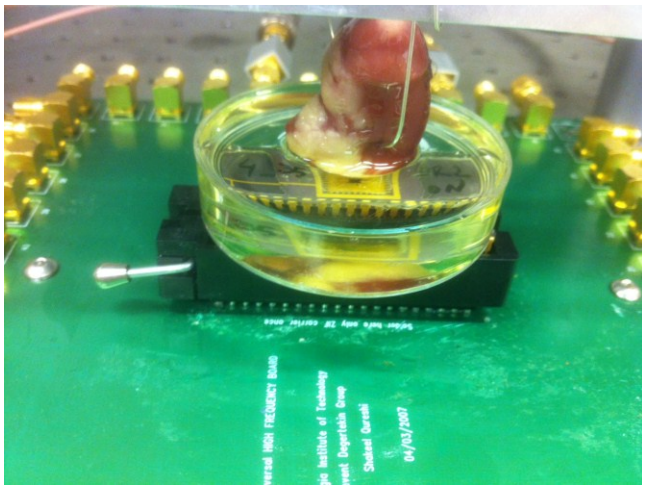

Figure 4. Experimental setup of wire-bonded CMUT array in a chip holder combined with a modified Petri dish for imaging a chicken heart phantom

where u_i and u_j is the 3-D vectors of transmit and receive in cartesian coordinates, respectively.

To suppress the sidelobes in the reconstructed images, we used a Cosine function applied radially on the aperture. In addition, we applied Norton's weighting function defined for ring arrays to obtain full disk resolution [5]. The weighting coefficients of Cosine apodization and Norton's weighting are expressed respectively as:

$$w_a(i,j) = 0.5\left(1 + \cos\left(\frac{\pi r_{ij}}{D_a}\right)\right), \qquad (3)$$

and

$$w_n(i,j) = 2\left|\sin(\theta_{ij})\right|, \qquad (4)$$

where r_{ij} is the length of the sum of corresponding transmit and receive element vectors, D_a is the diameter of effective aperture (coarray), θ_{ij} is the angle between transmit and receive element vectors.

For envelope detection, we used time-delay sampling technique to extract the quadrature component from the received signal that decreases computational time with respect to applying Hilbert transforms [9]. Following envelope detection, we applied logarithmic compression in a desired dynamic range to form the final image.

C. *Imaging Results from Phantom*

To demonstrate the potential of FL dual ring array for volumetric imaging, we used an ex-vivo chicken heart phantom. The phantom was immersed in oil inside the Petri dish and hanged 2.5 mm above the array surface as shown in Fig. 4. We collected 2688 RF A-scans from 56×48 Tx-Rx element combinations without using signal averaging. We reconstructed cross-sectional Bscan images in *yz* plane as well as 3-D volumetric image from the phantom data.

The *yz* plane Bscan image with 40 dB dynamic range is presented in Fig. 5. The image size is 10 mm in both dimensions. The brightest spot in the image is the reflection from the closest wall of chicken heart phantom to the array.

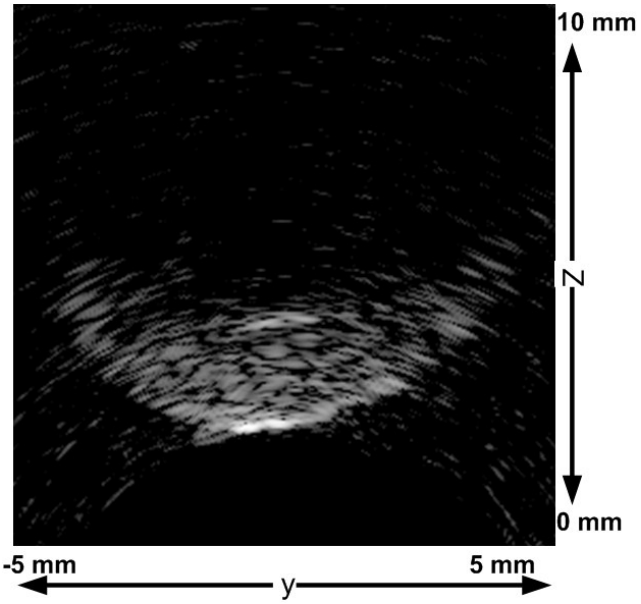

Figure 5. 2D Cross-sectional image of the chicken heart phantom. The image is displayed in a 40-dB dynamic range

Although, the aperture size of the CMUT array is too small compared to the phantom, the bottom curvature of the phantom is clearly visible in the Bscan image. In the image, a relatively weak second reflection can be seen back side of the phantom surface which is difficult to interpret since it is received from inside of the chicken heart. However, it can be a different boundary or a vessel passing through that cross-section. The computed experimental image SNR for the brightest location of the image is 56 dB. On the other hand, the theoretical overall image SNR is computed as 54dB including beamforming and single A-scan SNRs [10].

We also reconstructed a volume rendered image of the same phantom using the MicroView software of the GE Healthcare, as shown in Fig. 6. The volume rendered image is obtained in a 10 mm × 10 mm × 10 mm cubic volume. Similarly, the 3-D profile of the chicken heart phantom can be observed in the volumetric image. The data collection, for the whole array through 4 parallel receive channels takes around 16 ms and hence the theoretical image rate can be 62 frames per second.

IV. Conclusion

The imaging results demonstrate that the single-chip FL-IVUS system with monolithically integrated electronics has potential to visualize the front view of coronary arteries and produce true volumetric images which enables guiding interventions such as treatment of CTOs and helping stent deployment. Moreover, the system reduces fabrication and interconnection complexity as well as enabling miniaturization of FL-IVUS system.

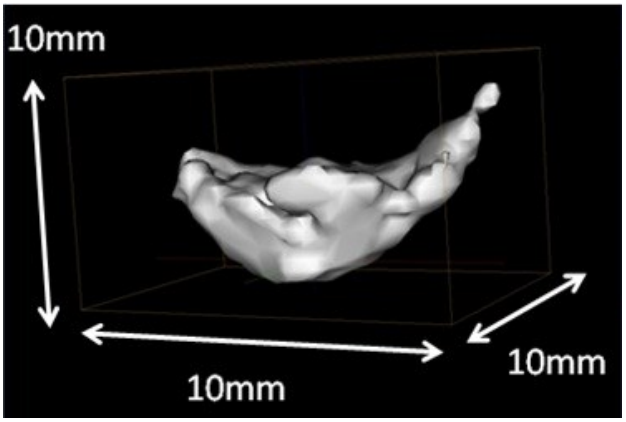

Figure 6. 3-D renedered volumetric image of the chicken heart phantom.

References

[1] A. van der Steen, R. A. Baldewsing, F. L. Degertekin, S. Emelianov, M. Frijlink, Y. Furukawa, D. Goertz, M. Karaman, P. Khuri-Yakub, K. Kim, F. Mastik, T. Moriya, O. Oralkan, Y. Saijo, J. Schaar, P. W. Serruys, S. Sethuraman, A. Tanaka, H. J. Vos, R. Witte, M. O'Donnell, "IVUS beyond the horizon," *EuroIntervention*, vol.2, pp.132-42, 2006.

[2] Y. Wang, D. N. Stephens, and M. O'Donnell, "A forward viewing ring-annular ultrasound array for intravascular imaging," in *Proc. IEEE Ultrason. Symp.*, pp. 1573–76, 2001.

[3] F. L. Degertekin, R.O. Guldiken, M. Karaman, "Annular-ring CMUT arrays for forward-looking IVUS: transducer characterization and imaging," *IEEE Trans. Ultrason., Ferroelect., Freq. Contr.*, vol. 53, pp.474-482, Feb. 2006.

[4] R. Guldiken, J. Zahorian, M. Balantekin, C. Tekeş, A. Sişman, M. Karaman, F. Levent Degertekin, "Dual-annular-ring CMUT array for forward-looking IVUS imaging," *Proc. of IEEE Ultrason. Symp.*, pp. 698-701,2006.

[5] D. T. Yeh, Ö. Oralkan, I. O. Wygant, M. O'Donnell, B.T. Khuri-Yakub, "3-D Ultrasound imaging using a forward-looking CMUT ring array for intravascular/intracardiac applications," *IEEE Trans. Ultrason., Ferroelect., Freq. Contr.,* vol. 53, no. 6, pp. 1202-1211, June 2006.

[6] G.Gurun, P. Hasler, L. Degertekin, "A 1.5-mm Diameter Single-Chip CMOS Front-End System with Transmit-Receive Capability for CMUT-on-CMOS Forward-Looking IVUS," *Ultrasonics Symposium (IUS), 2011 IEEE*, 2011.

[7] G.Gurun, P. Hasler, L. Degertekin, "Front-end receiver electronics for high-frequency monolithic CMUT-on-CMOS imaging arrays," *IEEE Transactions on Ultrasonics, Ferroelectrics and Frequency Control,* vol. 58, pp.1658-1668, 2011.

[8] J. Zahorian, M. Hochman, T. Xu, S. Satir, G. Gurun, M. Karaman, F. L. Degertekin, "Monolithic CMUT on CMOS Integration for Intravascular Ultrasound Applications," *IEEE Transactions on Ultrasonics, Ferroelectrics and Frequency Control,* vol. 58, no.12, pp.2659-2667, 2011.

[9] J. H. Kim, T. K. Song, and S. B. Park, "A pipelined sampled delay focusing in ultrasound imaging systems," *Ultrasonic Imaging,* vol. 9, pp. 75-91, 1987.

[10] J. A. Johnson, M. Karaman, B. T. Khuri-Yakub, "Coherent Array Imaging Using Phased Subarrays—Part I: Basic Principles," *IEEE Trans. Ultrason., Ferroelect., Freq. Contr.*, vol. 52, no. 1, pp. 37-50, 2005.